SUPPLEMENTAL METHODS AND FIGURE LEGENDS

Antibodies used in flow cytometry and analyzing strategies

PE- or PeCy7-anti-mouse CD62L (MEL-14, 1:200 dilution), PE-, PeCy5- or PeCy7-antimouse CD44 (IM7, 1:400), PE-, Biotin- or PeCy7-anti-mouse CD4 (GK1.5, 1:200), PE-, PeCy5- or Biotin- anti-mouse CD8α (53-6.7, 1:100), PE- or Biotin-anti-mouse TCRγδ (GL3, 1:100), Alexa Fluor 647-anti-mouse/rat Foxp3 (FJK-16s, 1:50) and PE-anti-mouse TCRβ (H57-597, 1:100) were purchased from eBioscience (San Diego, CA). Alexa Fluor 647-anti-mouse IL-17A (TC11-18H10.1, 1:250), PeCy7- or Pacific Blue anti-mouse CD45.1 (A20, 1:200), Alexa Fluor 647- or Alexa Fluor 700-anti-mouse CD45.2 (104, 1:100), Alexa Fluor 647-anti-mouse CD127 (A7R34, 1:100), PE- or PeCy7- or Biotin-anti-mouse CD3ε (145-2C11, 1:100), PE-CD25 (PC61, 1:100) and PE-KLRG1 (2F1/KLRG1, 1:100) were from Biolegend (San Diego, CA). APC-anti-mouse IL-10 (JES5-16E3, 1:100), FITC-anti-human CD3 (UCHT1, 1:50), PeCy7-anti-human CD4 (SK3, 1:50) and Streptavidin-PE-Texas Red (1:200) were from BD Biosciences (San Jose, CA). PE-anti-human CCR10 (314305, 1:10) was from R&D Systems (Minneapolis, MN). PE-Alexa Fluor 610-anti-mouse CD4 (RM4-5, 1:100) and PE-Alexa Fluor 610-anti-mouse CD8α (5H10, 1:100) were from Invitrogen (Camarillo, CA). Foxp3/Transcription Factor Staining Buffer Set was from eBioscience (San Diego, CA). Cells stained with proper combination of antibodies and analyzed on flow cytometer FC500 (Beckman Coulter) or BD Fortessa LSRII (San Jose, CA). Cells stained with a single individual antibody were used to calibrate the signal output and compensation. Staining with the isotype control antibodies was included to confirm the specific signal for their corresponding antigen-specific antibody staining. Flow data were analyzed with Flowjo (Ashland, OR).

Figure E1. (A) Ear thickness changes of $CCR10^{-/-}$ and $CCR10^{+/-}$ mice after the one-time topical application of indicated concentrations of TPA on the ear. N≥6. **(B)** Quantitative real-time RT-PCR analysis of RNA isolated from treated ears 3 days after the one-time TPA application for TNF-α, IL-1β and IL-10. "No" indicates untreated skin samples. The values are relative levels normalized on β-actin. N= 4 $CCR10^{+/-}$ and 5 $CCR10^{-/-}$ mice.

Figure E2. Representative flow cytometric analysis of gated lymphocytes isolated from the skin of $CCR10^{+/-}$ and $CCR10^{-/-}$ mice for $CD3^{+}TCR\beta^{+}$ T cells and their expression of EGFP (CCR10).

Figure E3. Representative flow cytometric analysis of gated $EGFP^{+}$ $CD4^{+}$ and $CD8^{+}$ T cells isolated from the skin of $CCR10^{+/-}$ and $CCR10^{-/-}$ mice for molecular markers associated with the T cell memory.

Figure E4. Representative FACS analysis of gated splenic $CD3+CD8^{+}$ (top) and $CD3+CD4^{+}$ (bottom) T cells for $EGFP^{+}$ subsets in $CCR10^{-/-}$ and $CCR10^{+/-}$ mice.

Figure E5. (A) Representative flow cytometric analysis of gated skin T cell populations (indicated in the figure) for their $CCR10^{-/-}$ vs. $CCR10^{+/-}$ bone marrow origins in irradiated wild type recipients two months after the BM transfer. CD45.1 and CD45.2 polymorphism was used to distinguish T cells of different donor and host origins. Total splenic T cells were analyzed for their $CCR10^{-/-}$ vs. $CCR10^{+/-}$ bone marrow origins and used as the normalized reference to corresponding skin T cell populations. **(B)** Relative contribution of transferred $CCR10^{-/-}$ vs. $CCR10^{+/-}$ BM cells to the indicated EGFP- skin T cell subsets in irradiated WT recipient mice. N=5 each.

Figure E6. (A) Representative FACS analysis of gated $CD3^{+}CD4^{+}$ T cells of TPA-treated ear skin of $CCR10^{+/-}$ and $CCR10^{-/-}$ mice for $EGFP^{+}$ and $EGFP^{-}$ Treg cells. TPA (33μg/ml) was topically applied to ears. Two days after the TPA application, cells isolated from treated ears were analyzed. **(B)** Average percentages of $EGFP^{+}$ and

EGFP^{-} Treg cells of total CD4^{+} T cells isolated from TPA-treated ear skin of CCR10$^{+/-}$ and CCR10$^{-/-}$ mice based on the analysis in panel A. N=3 each.

Figure E7. CCR10 is critical in localization of CCR10^{+} CD4+ OT-II T cells into homeostatic skin. **(A-B)** Flow cytometry of gated CD3+CD4+ OT-II cells isolated from Ova-treated inflamed ear skin **(A)** and untreated torso skin **(B)** for their expression of EGFP. **(C)** Average percentages of CCR10+/- and CCR10-/- OT-II T cells of the inflamed ear skin and un-inflamed torso skin that express EGFP (CCR10). N=3 each.

Figure E8. Representative flow cytometric analysis of T cells isolated from *L. major*-infected ears of CCR10$^{-/-}$ vs. CCR10$^{+/-}$ mice for different T subsets and their expression of EGFP. The mice were analyzed one month after the infection.

Figure E9. A schematic illustration of roles of CCR10 in regulation of skin Treg and Teff cells under homeostatic conditions.

SUPPLEMENTAL FIGURES

Figure E1. (A) Ear thickness changes of CCR10$^{-/-}$ and CCR10$^{+/-}$ mice after the one-time topical application of indicated concentrations of TPA on the ear. N≥6. **(B)** Quantitative real-time RT-PCR analysis of RNA isolated from treated ears 3 days after the one-time TPA application for TNF-α, IL-1β and IL-10. "No" indicates untreated skin samples. The values are relative levels normalized on β-actin. N= 4 CCR10$^{+/-}$ and 5 CCR10$^{-/-}$ mice.

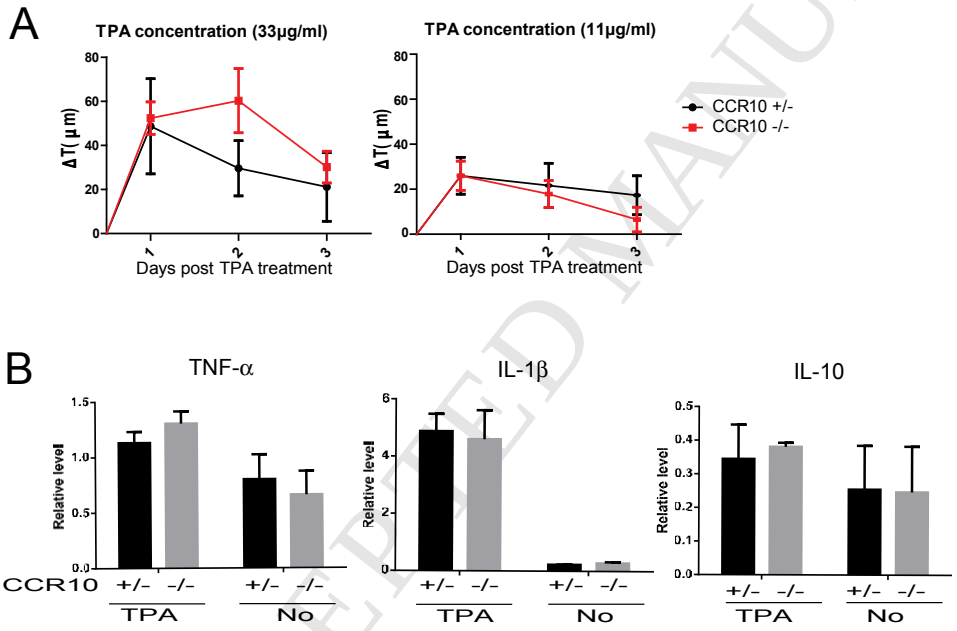

Figure E2. Representative flow cytometric analysis of gated lymphocytes isolated from the skin of CCR10$^{+/-}$ and CCR10$^{-/-}$ mice for CD3^{+}TCRβ^{+} T cells and their expression of EGFP (CCR10).

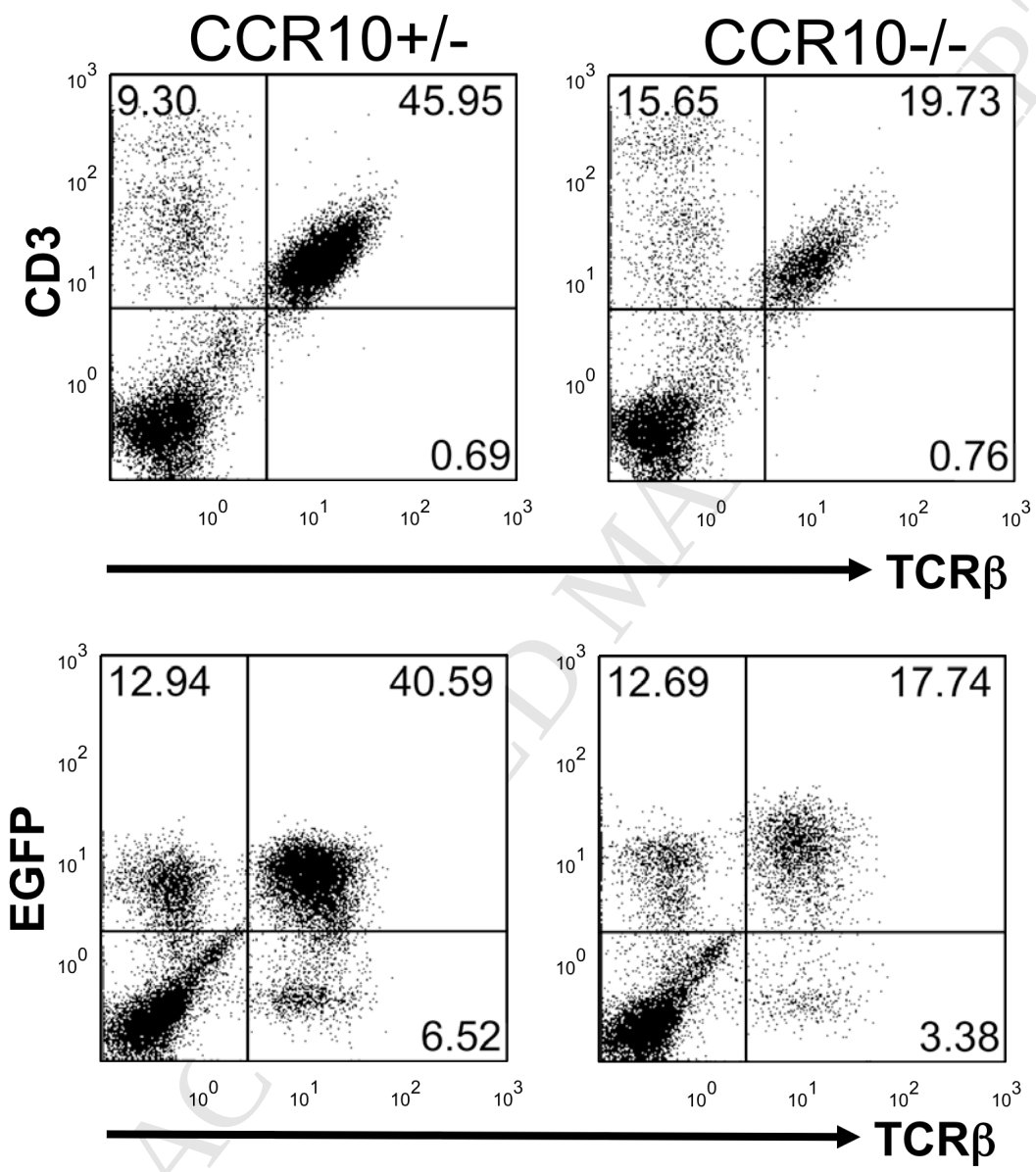

Figure E3. Representative flow cytometric analysis of gated EGFP^{+} CD4^{+} and CD8^{+} T cells isolated from the skin of CCR10$^{+/-}$ and CCR10$^{-/-}$ mice for molecular markers associated with the T cell memory.

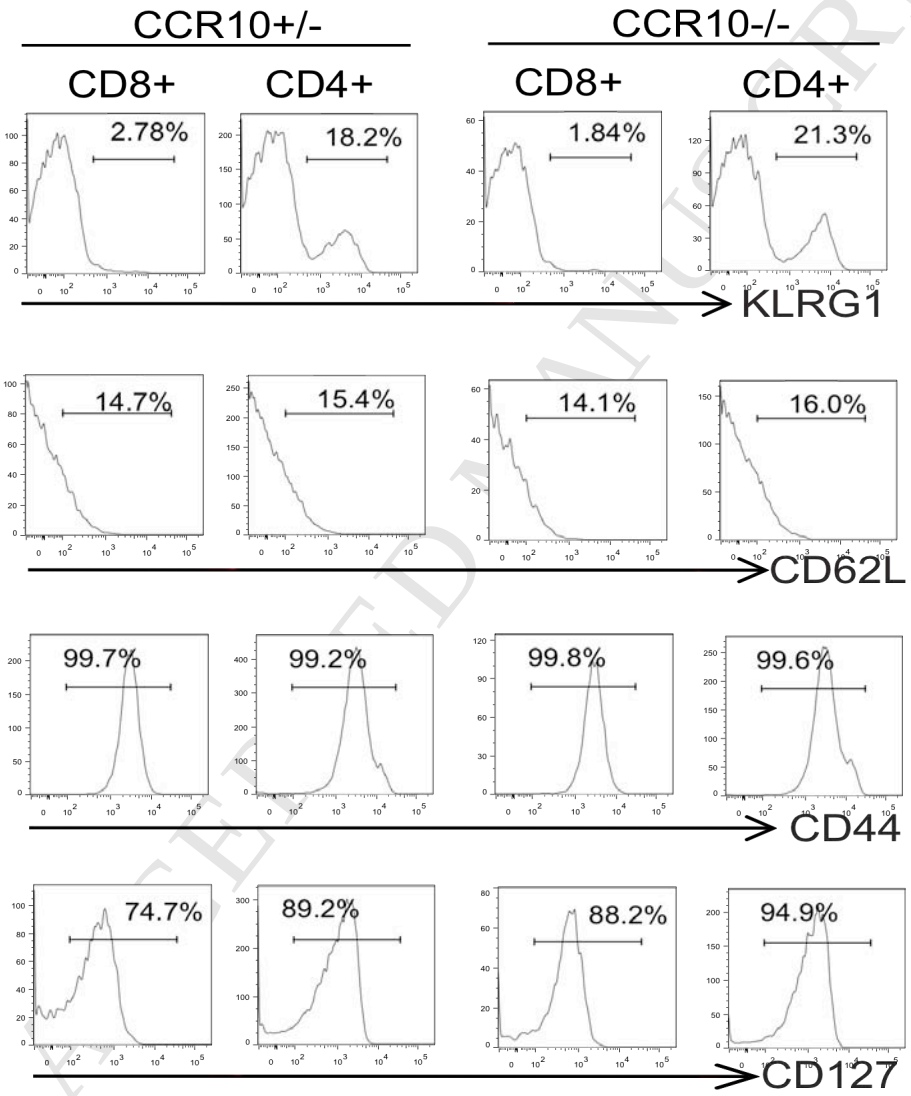

Figure E4. Representative FACS analysis of gated splenic CD3+CD8^{+} (top) and CD3+CD4^{+} (bottom) T cells for EGFP^{+} subsets in CCR10$^{-/-}$ and CCR10$^{+/-}$ mice.

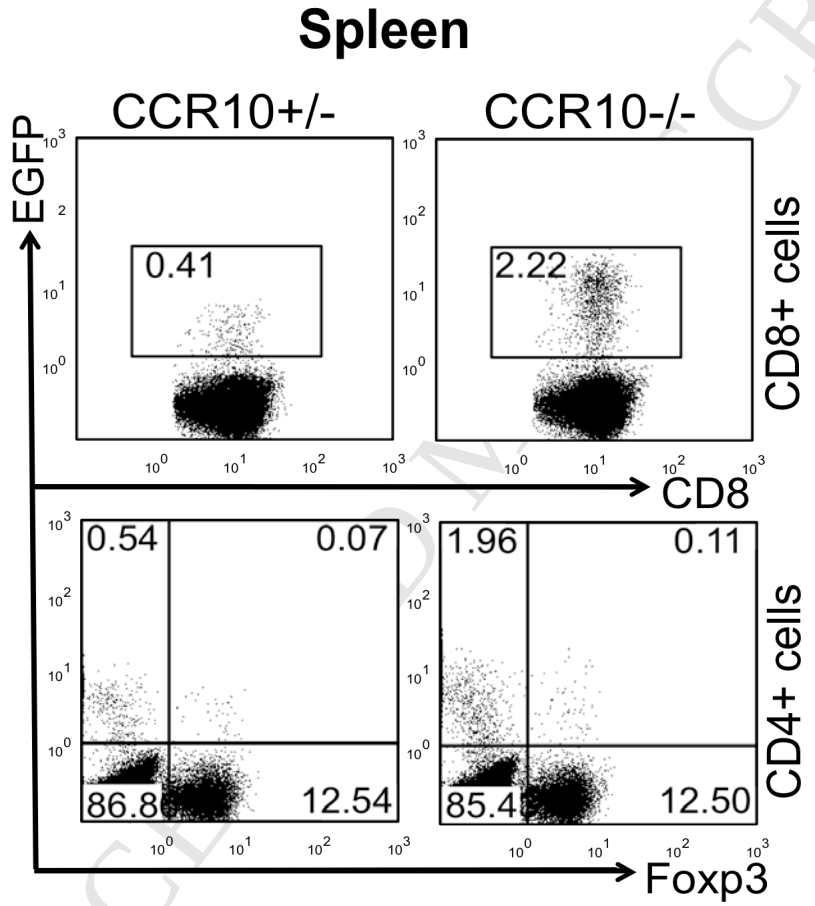

Figure E5. (A) Representative flow cytometric analysis of gated skin T cell populations (indicated in the figure) for their CCR10$^{-/-}$ vs. CCR10$^{+/-}$ bone marrow origins in irradiated wild type recipients two months after the BM transfer. CD45.1 and CD45.2 polymorphism was used to distinguish T cells of different donor and host origins. Total splenic T cells were analyzed for their CCR10$^{-/-}$ vs. CCR10$^{+/-}$ bone marrow origins and used as the normalized reference to corresponding skin T cell populations. **(B)** Relative contribution of transferred CCR10$^{-/-}$ vs. CCR10$^{+/-}$ BM cells to the indicated EGFP^{-} skin T cell subsets in irradiated WT recipient mice. N=5 each.

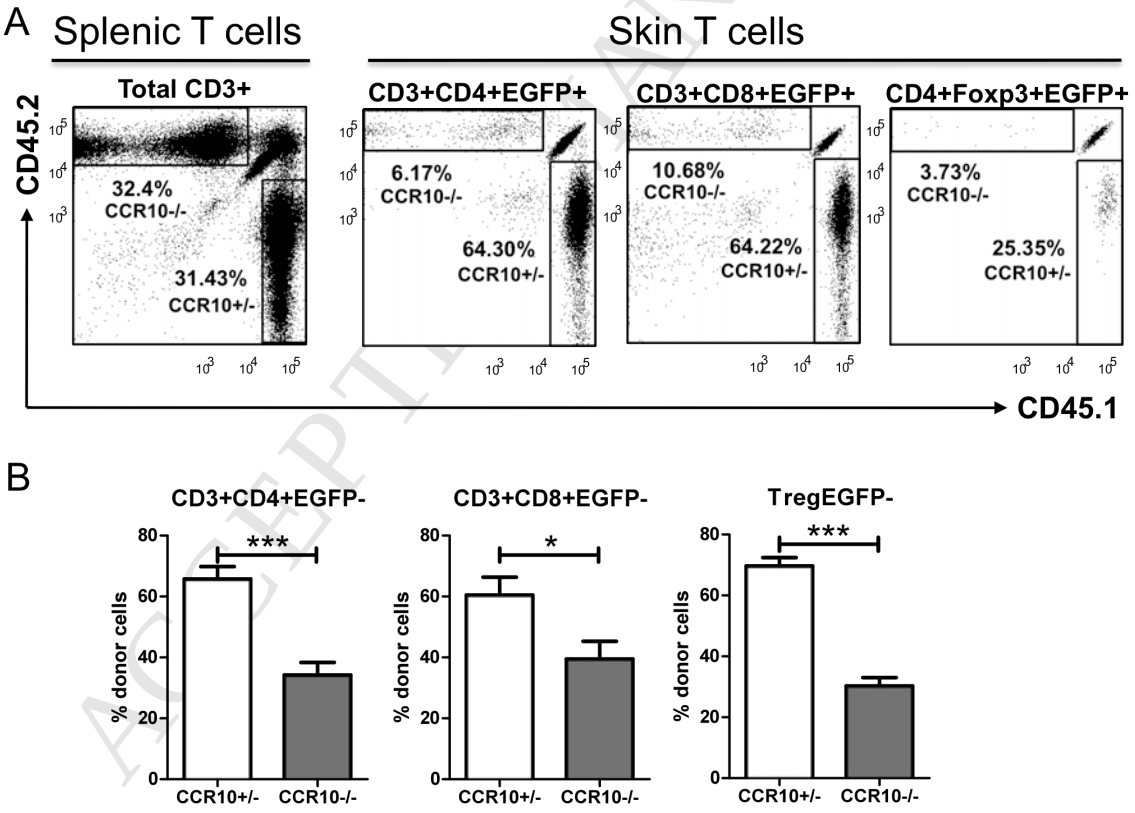

Figure E6. (A) Representative FACS analysis of gated $CD3^+CD4^+$ T cells of TPA-treated ear skin of $CCR10^{+/-}$ and $CCR10^{-/-}$ mice for $EGFP^+$ and $EGFP^-$ Treg cells. TPA (33μg/ml) was topically applied to ears. Two days after the TPA application, cells isolated from treated ears were analyzed. **(B)** Average percentages of $EGFP^+$ and $EGFP^-$ Treg cells of total $CD4^+$ T cells isolated from TPA-treated ear skin of $CCR10^{+/-}$ and $CCR10^{-/-}$ mice based on the analysis in panel A. N=3 each.

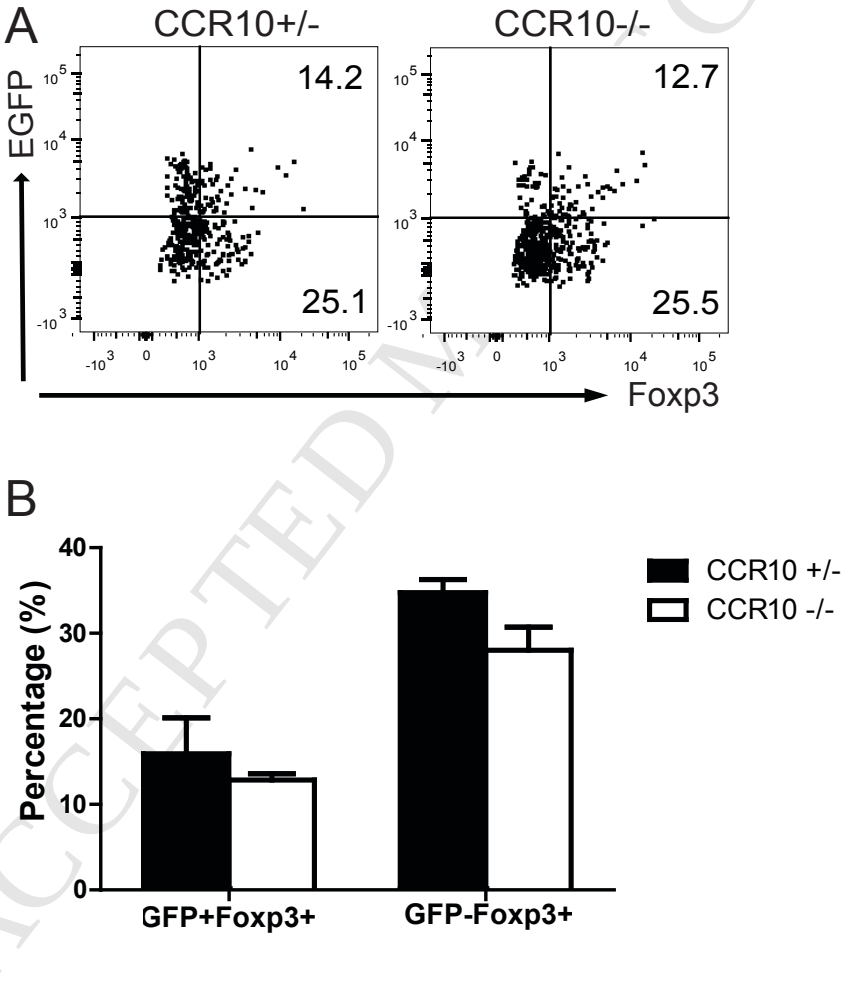

Figure E7. CCR10 is critical in localization of CCR10^{+} CD4+ OT-II T cells into homeostatic skin. **(A-B)** Flow cytometry of gated CD3+CD4+ OT-II cells isolated from Ova-treated inflamed ear skin (A) and untreated torso skin (B) for their expression of EGFP. **(C)** Average percentages of CCR10+/- and CCR10-/- OT-II T cells of the inflamed ear skin and un-inflamed torso skin that express EGFP (CCR10). N=3 each.

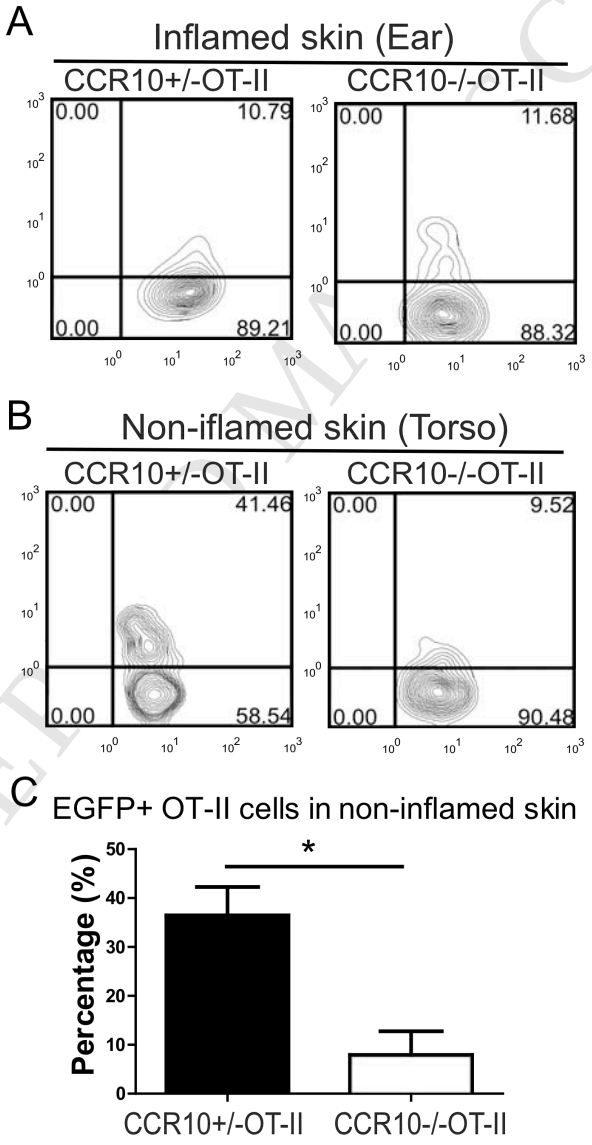

Figure E8. Representative flow cytometric analysis of T cells isolated from *L. major*-infected ears of CCR10$^{-/-}$ vs. CCR10$^{+/-}$ mice for different T subsets and their expression of EGFP. The mice were analyzed one month after the infection.

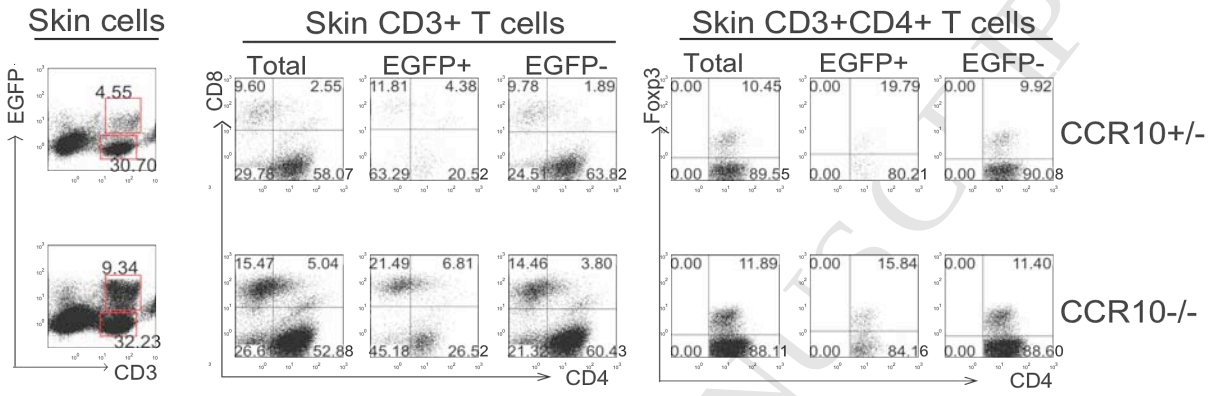

Figure E9. A schematic illustration of roles of CCR10 in regulation of skin Treg and Teff cells under homeostatic conditions.